Vol. 502: 145–156, 2014
doi: 10.3354/meps10720

MARINE ECOLOGY PROGRESS SERIES
Mar Ecol Prog Ser

Published April 15

Positive and negative responses of coral calcification to elevated pCO_2: case studies of two coral species and the implications of their responses

Hui Huang[1,2], Xiang-Cheng Yuan[1,*], Wei-Jun Cai[3], Cheng-Long Zhang[1], Xiubao Li[1], Sheng Liu[1]

[1]Key Laboratory of Tropical Marine Bio-resources and Ecology, South China Sea Institute of Oceanology, Chinese Academy of Sciences (CAS), Guangzhou, PR China

[2]Tropical Marine Biological Research Station in Hainan, CAS, Sanya 572000, PR China

[3]School of Marine Science and Policy, University of Delaware, Newark, Delaware 19716, USA

ABSTRACT: Fragments of 2 coral species (*Acropora nasuta* and *Pocillopora damicornis*), collected from the South China Sea, were incubated for 94 d under controlled conditions of pCO_2 = 389, 700, and 1214 µatm. Our incubation experiments showed that the net calcification rate of *A. nasuta* responded negatively to elevated pCO_2 in both short and mid-term incubations. In contrast, the net calcification rate of *P. damicornis* increased under elevated pCO_2 during the first 17 d, but then returned to background rates. Based on previous models, our modified models showed that the different responses of these 2 coral species depended on the dissolved inorganic carbon (DIC) and pH levels in coral calcifying fluid. In the studied models, the positive responses of coral calcification to higher pCO_2 could be explained by either low DIC due to a higher photosynthesis rate or a stronger H^+ pump. If DIC in calcifying fluid is greatly reduced by photosynthesis, the decreased DIC in calcifying fluid may be benefited by enhanced external seawater CO_2, which will partially offset the dissolution due to ocean acidification. Therefore, in addition to our experimental results, our model provides a theoretical basis showing how coral may respond negatively and positively to ocean acidification.

KEY WORDS: Coral calcification · Ocean acidification · Dissolved inorganic carbon · pH · Modelling

INTRODUCTION

In the past several decades, human activities, especially the combustion of fossil fuels, have dramatically increased atmospheric pCO_2 (IPCC 2007). About 30% of the anthropogenic CO_2 released annually is absorbed by the ocean (Feely et al. 2004). This absorption leads to ocean acidification and a decrease in ocean pH, with accompanying declines in carbonate ion (CO_3^{2-}) concentration and aragonite saturation state (Ω_A) (Kleypas et al. 2006, Hoegh-Guldberg et al. 2007). Since coral calcification is believed to be largely controlled by the degree of Ω_A, elevated pCO_2 will significantly decrease the coral net calcification rate (Langdon & Atkinson 2005, Kleypas et al. 2006, Cohen & Holcomb 2009). Hence, there have been widespread concerns about the future of our oceans in a high-CO_2 world (Hoegh-Guldberg et al. 2007), including the likelihood of coral reef decline.

There have been a number of field and laboratory experiments investigating the impact of ocean acidification on coral calcification rates, but our understanding of the effect of elevated pCO_2 on calcification is still relatively limited (Langdon & Atkinson 2005, Kleypas & Yates 2009). Some studies have revealed that marine calcifiers exhibit a broad spec-

*Corresponding author: xcyuan@scsio.ac.cn

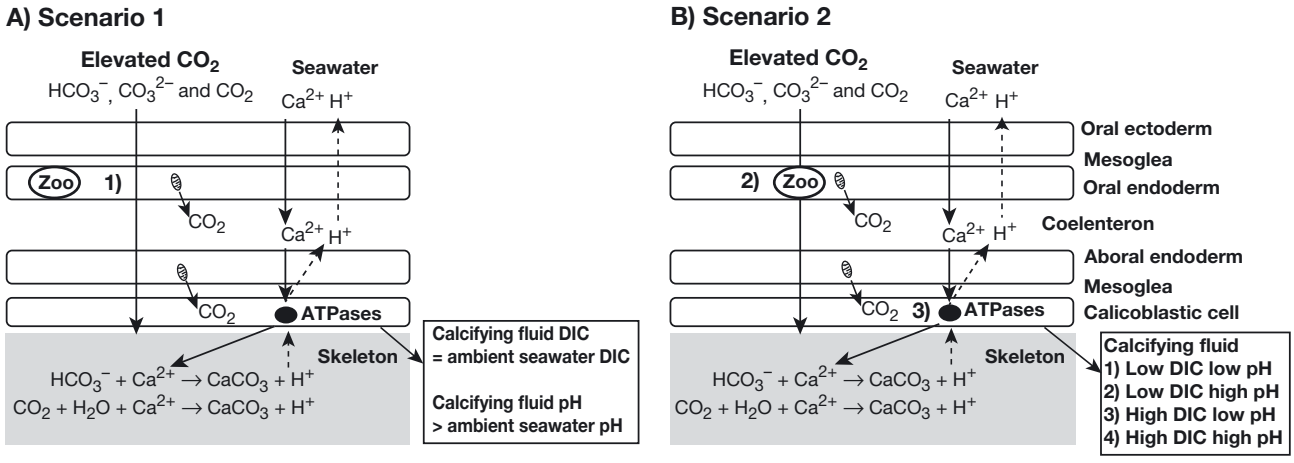

Fig. 1. Schematic representation of 2 scenarios for dissolved inorganic carbon (DIC) in calcifying fluid. (A) Scenario 1: DIC in calcifying fluid is equal to that in the seawater; (B) Scenario 2: DIC and pH in calcifying fluid are modified by coral photosynthesis and respiration. There are 3 possible pathways by which elevated CO_2 can affect coral calcification: (1) directly increase DIC in calcifying fluid by enhancing CO_2 diffusion; (2) regulating coral photosynthesis and respiration; and (3) regulating H^+ flux between the external seawater and the calcifying fluid. Zoo: zooxanthella; ATPases: ion pumping enzymes

trum of calcification responses to CO_2-induced ocean acidification, including negative, threshold-negative, neutral, threshold-positive, and parabolic responses (Ries 2011, Wicks & Roberts 2012). The sensitivity to increased CO_2 differs substantially both within and among species. However, there are relatively few studies that compare and explore the contrasting responses of calcification rates to CO_2-induced ocean acidification among different species. Hence, the mechanisms behind the positive or negative effects of ocean acidification on coral calcification are still poorly understood.

There are several theories about biological control of coral calcification. Ca^{2+} and inorganic carbon can be delivered into the calcifying fluid located between calicoblastic cells and the skeleton, and H^+ can be removed from the calcifying fluid (Fig. 1) (McConnaughey & Whelan 1997, Furla et al. 2000, Al-Horani et al. 2003). In addition, CO_2 is assumed to freely diffuse from the seawater, the coelenteron, and the calcifying fluid into the polyp tissue and out again (Hohn & Merico 2012). A bicarbonate transporter (co-transport of HCO_3^- and H^+) has been proposed by Furla et al. (2000) and appears to be responsible for active carbon uptake from the tissue into the calcifying fluid. The pathway by which elevated CO_2 affects calcification in calcifying fluid is still unclear. Here, we suggest that there are at least 3 possible pathways by which elevated CO_2 can affect coral calcification (Fig. 1): (1) directly enhancing the dissolved inorganic carbon (DIC) concentration by diffusion of CO_2 into calcifying fluid; (2) regulating coral photosynthesis and respiration and thus indirectly influencing DIC concentration in calcifying fluid; and (3) regulating H^+ flux from calcifying fluid (Ries 2011). The effects of the second pathways seem to be variable among coral species, as elevated CO_2 can result in variable responses of coral photosynthesis, which may depend on different phylotypes of *Symbiodinium* (Brading et al. 2011). Crawley et al. (2010) reported that elevated CO_2 could induce a decrease in zooxanthellae photorespiration and productivity, but some other studies showed that there was no direct effect of increased CO_2 on the rates of coral or reef community photosynthesis (Langdon et al. 2003, Schneider & Erez 2006, Marubini et al. 2008). In addition, the third pathway has been supported by Ries (2011), who suggested that the coral removes less H^+ from its calcifying fluid under acidified conditions to maintain stable external:internal H^+ ratios between the external seawater and the calcifying fluid.

Coral reefs in the South China Sea are widely distributed around many islands (e.g. Hainan, Weizhou, Nansha, and Xisha Islands) and represent 5% of the global coral reef area (Zhang 2007). A recent model showed that coral calcification rates in the Nansha Islands have declined by ~12% in the past 30 yr and suggested that they will further decline by 26% and 33% in 2065 and 2100, respectively, relative to the pre-industrial period (Zhang & Chen 2006). More severely, coral abundance has declined by at least 80% over the past 30 yr on coastal fringing reefs along the Chinese mainland and adjoining Hainan Island (Hughes et al. 2012). If pH continues to decrease, serious impacts on the Sanya coral reef ecosystems of Hainan Island can be expected due to the

combined effects of disparate anthropogenic factors, such as eutrophication, urbanization, marine aquaculture, and overfishing (Zhang 2012).

The coral species *Acropora* and *Pocillopora* are widespread throughout the tropical Indian, Pacific, and western Atlantic Oceans (Wallace 1999, Manzello 2010) and are coexisting and dominant in Sanya Bay. *Pocillopora damicornis* is the most important reef builder in the eastern tropical Pacific (Manzello 2010). In Panamá, its linear extension declined significantly by nearly one-third from 1974 to 2006, partly due to ocean acidification (Manzello 2010). However, the effects of ocean acidification on Pacific *Acropora nasuta* have not been studied yet. In the present study, these 2 coral species were selected (1) to examine the impacts of CO_2-induced ocean acidification on calcification rates and (2) to investigate the effects of ocean acidification on calcification rates using a model of calcification that incorporates the effects of photosynthesis and respiration on calcifying fluid DIC.

Table 1. Values of pCO_2, pH, temperature (T), salinity, total alkalinity (TA), dissolved inorganic carbon (DIC), and aragonite saturation state (Ω_A) during 94 d incubations. All values are means ± SD

pCO_2 (µatm)	pH	T (°C)	Salinity	TA (µmol l^{-1})	DIC (µmol l^{-1})	Ω_A
389±24	8.03±0.14	27±2	34±0.02	2219±26	1902±32	3.4±0.06
700±75	7.82±0.16	27±2	34±0.02	2225±45	2021±87	2.4±0.08
1214±102	7.61±0.18	27±2	34±0.02	2224±31	2110±96	1.6±0.10

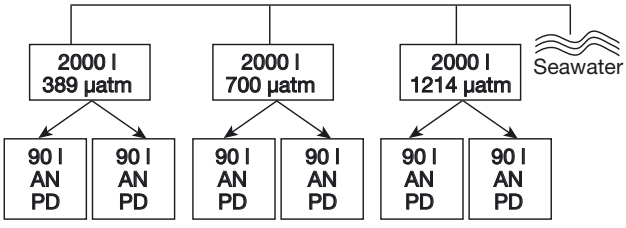

Fig. 2. Experimental design. Seawater from Sanya Bay was pumped through a pipeline into three 2000 l tanks. The natural seawater enriched with different pCO_2 levels was redistributed into six 90 l glass aquaria from these three 2000 l tanks. Coral species *Acropora nasuta* (AN, n = 10 to 12) and *Pocillopora damicornis* (PD, n = 5 to 8) were incubated in the same 90 l glass aquaria with replicates in 3 treatments of different pCO_2 levels (389, 700, and 1214 µatm)

MATERIALS AND METHODS

Coral collection

Two coral species, *Acropora nasuta* and *Pocillopora damicornis*, were collected near our field laboratory from a reef in Sanya Bay (18.15°N, 109.30°E). The mean annual sea surface temperature (SST) there is 27°C (20.5 to 30.9°C) (Li et al. 2008). These coral species were collected at depths of ~3 to 6 m in July 2010 and divided into 2 to 10 fragments. Epiphytes, associated fauna, and other detritus were carefully removed from all fragments. Each fragment was suspended in seawater and weighed (see 'Buoyant weight method'), and the initial weight of each coral fragment ranged from 4 to 6 g.

Water supply and CO_2 enrichment

The experiments were conducted outside the Tropical Marine Biological Research Laboratory in Sanya Bay, Hainan Island. The laboratory was supplied with running seawater drawn from a depth of 5 m in the bay. Seawater was pumped through a pipeline with a sand filter and distributed into three 2000 l tanks (Fig. 2), through which seawater was bubbled with CO_2 gas from a high-pressure CO_2 cylinder. CO_2 gas-flow rates were regulated using high-precision pressure gauges and valves (DC01-01, Dici) to achieve 3 targeted pH values (pH_T = 8.03, 7.82, and 7.61) (Table 1). These pH values correspond to the designated pCO_2 levels (389, 700, and 1214 µatm) (Table 1) that were projected for the pCO_2 levels of the present, the end of the present century, and next century. Then, a 2 × 3 experiment was set up using the 6 independent aquaria, enriched with the natural seawater of 3 different pCO_2 levels (Fig. 2). A total of 5 to 12 coral fragments of each species were suspended in each glass aquaria.

The inflow rates of seawater were adjusted to ~1.5 l min^{-1}, which resulted in a turnover time of ~1 h in all aquaria. Stable pH conditions (replicates within ±0.15 pH units) were achieved within ~2 d by adjusting CO_2 and water flow rates. Since retaining the natural diurnal variations in some parameters (e.g. pH) was desired in the mesocosms, diurnal variations in pH of ±0.15 in all aquaria were allowed. The ranges of pH values during the 94 d incubation are presented in Table 1.

Coral culture

The coral fragments were allowed to acclimate for 2 to 3 wk in each fiberglass aquarium (90 l) before the

start of the experiment. After this period, coral fragments were randomly assigned to 1 of the 3 treatments (at pCO_2 levels of 389, 700, and 1214 µatm). Coral fragments were attached to nylon strings and suspended in these glass aquaria (90 l) for 110 d. Buoyant weights were measured on Days 17 and 94 to calculate daily calcification rates (see 'Buoyant weight method').

In addition to continuously renewing the water with natural seawater, we cleaned each aquarium every week to prevent the growth of fouling organisms and accumulation of detritus. Due to the continuous seawater renewal, all parameters (e.g. salinity, temperature, irradiance, pH, and alkalinity) varied with natural conditions in Sanya Bay. Since the sampled corals grew at ~20 to 60% of surface light in natural seawater at depths of 3 to 6 m, each aquarium was covered with a neutral density filter to provide a light field that was ~50% of the surface irradiance.

Analysis of PAR, salinity, and temperature

Photosynthetically active radiation (PAR) at the surface and the sampling depths was measured using a quantum sensor (model LI-192 SA, LI-COR) and a data logger (Li-1400, LI-COR). Salinity and temperature were measured using a conductivity probe (Orion 013010MD) with precisions of ±0.1 psu and ±0.1°C (Table 1). Typical diurnal variations in PAR in summer and autumn are shown in Fig. 3.

Analysis of pH and alkalinity

Variations in the pH in all aquaria were monitored routinely every 3 to 24 h to ensure that pH was relatively constant in all aquaria (Table 1). Diurnal variations of pH and alkalinity in natural seawater have been reported by Zhang et al. (2013). pH was measured using a Ross semi-micro combination pH glass electrode (Orion 8103BNUWP) that was calibrated using the buffer (a 2-amino-2-hydroxymethyl-1,3-propanediol [Tris] buffer at salinity 35) as described in SOP 6a (Dickson et al. 2007). The precision of the pH measurement was ±0.005.

For total alkalinity (TA) measurements, seawater samples (250 ml) were poisoned with 50 µl of saturated $HgCl_2$ and stored in BOD bottles in the dark at 4°C until analysis. They were measured within 1 to 2 d using an automated titration system (Metrohm 877 Titrino plus) at ~25°C following SOP 3b (Dickson et al. 2007). The HCl titrant solution (0.1 M) was calibrated against certified reference materials (Batch 101#) from the laboratory of Dr. Andrew Dickson. Analysis of duplicate samples suggested that our titration had a precision of ±2 µM.

The other carbonate system parameters, including total DIC, pCO_2, and the Ω_A, were calculated using the CO2SYS program (Lewis et al. 1998). Carbonate dissociation constants K_1 and K_2 (Roy et al. 1993) and the aragonite solubility product (K_{sp}) (Mucci 1983) were used in our calculations. The ranges of DIC, pCO_2, and Ω_A values during the 94 d incubation are presented in Table 1.

Buoyant weight method

Calcification rates were measured using the buoyant weight technique (Spencer Davies 1989). An electronic balance (AUY220) with a precision of ±1 mg was used to weigh corals with a hook at the bottom. The fragments were carefully cleaned of epiphytes and detritus before each measurement. In all treatments, each fragment was weighed at the beginning as well as on Days 17 and 94. The net calcification rates were estimated as the weight change between the 2 times of weighing per initial weight per day (Spencer Davies 1989).

Skeletal $\delta^{13}C$ and $\delta^{18}O$ analysis

After coral tissue was removed using an airbrush, 200 to 250 µg surface skeleton was powdered. Samples were acidified in dried concentrated phosphoric acid (H_3PO_4). Surface skeletal $\delta^{13}C$ and $\delta^{18}O$ were analyzed following standard procedures on a Finni-

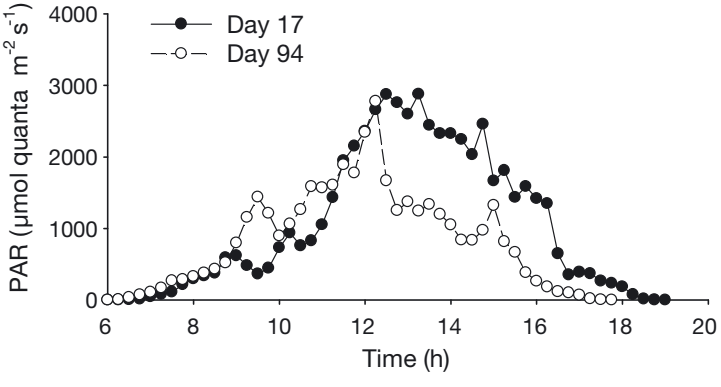

Fig. 3. Diurnal variations in photosynthetically active radiation (PAR), measured above the experimental aquaria, on Days 17 (summer) and 94 (autumn)

gan MAT mass spectrometer in the East China Normal University, and analytical precision and reproducibility were monitored using a laboratory working standard introduced in-between samples. The oxygen and carbon isotope compositions are expressed as $\delta^{13}C$ and $\delta^{18}O$ relative to the Vienna PDB standard. The precision for oxygen and carbon isotopes was better than 0.08‰ and 0.05‰, respectively.

Modeling

To understand the mechanisms of coral responses to elevated pCO_2 more fully, we modified the model of Ries (2011) for 2 scenarios. In both scenarios, we set temperature = 25°C, salinity = 34, external seawater alkalinity = 2200 µM, and atmospheric pressure = 1.015 atm.

Scenario 1: constant DIC. Scenario 1 showed how Ω_A in calcifying fluid responded to different levels of pCO_2, assuming that the calcifying fluid's DIC was equivalent to the DIC of the external seawater, as was assumed by Ries (2011). TA at the site of calcification was calculated as the external seawater's alkalinity (2200 µmol l^{-1}) plus the H^+ concentrations removed from the calcifying fluid, assuming H^+ removal worked to maintain fixed external:internal H^+ ratios (e.g. 7:1, 45:1, 90:1, 200:1, and 300:1) (see details in Ries 2011).

Scenario 2: varying DIC due to photosynthesis and respiration. Calcifying fluid DIC is not necessarily equivalent to the DIC concentration in the external seawater, as it is possible that DIC is added to the calcifying fluid via respiration or removed via photosynthesis. Hence, modeling Scenario 2 allowed us to examine how Ω_A in the calcifying fluid would respond to different levels of net DIC deviation (ΔDIC) in the coral's coelenteron or adjacent surface microenvironments under external pCO_2 values of 389, 700, and 1214 µatm, with different H^+ pumping resulting in external:internal H^+ ratios ($[H^+]_E/[H^+]_I$) of 7:1 (weak pumping) or 100:1 (strong pumping). Since coral photosynthesis and respiration varied broadly (see 'Discussion'), net ΔDIC values of −2000 to 2000 µmol l^{-1} were used in our simulations.

Table 2 summarizes the carbonate system parameters used to calculate the pH and Ω_A in the calcifying fluid that vary with different levels of atmospheric pCO_2. Table 2 also shows an example of model calculation when the external:internal H^+ ratio is 7:1. Briefly, we assume ΔDIC is mainly caused by photosynthesis and respiration, and the small TA change due to photosynthesis (Cai et al. 2011) is not included in our model. Thus, the pH in coelenterons can be calculated from DIC and TA. The pH in calcifying fluid can be estimated from the TA based on a proposed external:internal H^+ ratio and a DIC equal to that in coral coelenterons. Finally, Ω_A could be esti-

Table 2. Carbonate system constraints varying with different pCO_2 levels of 389, 700, and 1214 µatm. The external:internal H^+ ratio of 7:1 was selected as an example to show how these carbonate system constraints were calculated. (Note: only −1000, −200, 200, and 1000 µmol l^{-1} ΔDIC are presented, although we assumed the range is −2000 to 2000 µmol l^{-1}.) ΔDIC: net dissolved inorganic carbon (DIC) deviation due to photosynthesis and respiration; Ω_A: saturation state of aragonite in calcifying fluid, calculated based on DIC and pH. In the coelenteron, DIC is the DIC in ambient seawater + ΔDIC, which is the DIC concentration in coral coelenterons or adjacent surface microenvironments, and pH is the pH in coelenterons or adjacent surface microenvironments, assuming that TA did not change due to photosynthesis and respiration. In the calcifying fluid, DIC was assumed to come from DIC in coral coelenterons or adjacent surface microenvironments, and pH in the calcifying fluid was calculated based on an external:internal H^+ ratio of 7:1

Ambient seawater				Coelenteron			Calcifying fluid (7:1)		
pCO_2	TA	pH	DIC	ΔDIC	DIC	pH	DIC	pH	Ω_A
389	2200	8.18	1904	−1000	904	9.68	904	10.53	13.9
				−200	1704	8.48	1704	9.32	17.4
				200	2104	7.74	2104	8.59	8.3
				1000	2904	6.48	2904	7.33	0.8
700	2200	7.97	2013	−1000	1013	9.46	1013	10.31	15.5
				−200	1813	8.32	1813	9.17	18.3
				200	2213	7.42	2213	8.27	6.3
				1000	3013	6.42	3013	7.27	1.0
1214	2200	7.53	2133	−1000	1133	9.13	1133	9.98	16.5
				−200	1933	8.01	1933	8.85	13.4
				200	2333	6.96	2333	7.80	2.4
				1000	3133	6.21	3133	7.05	0.6

mated similarly based on the calculated DIC and pH in calcifying fluid.

Statistical analyses and calculations

To test the effects of pCO_2 on coral calcification, a partially nested ANOVA was used, in which pCO_2 was a fixed effect and tank was a random effect nested in pCO_2. All data were normally distributed according to plots of residuals versus predicted values for each variable or were transformed to meet the condition of normality. The error bars for the bioassay represented a pooled sample standard deviation of the means. A significance level of $p < 0.05$ was used to determine statistical differences. All statistical analyses were performed using the statistical software SPSS (SPSS Inc.).

RESULTS

Effects of elevated pCO_2 on coral calcification

After 110 d, there was 13% coral mortality in the treatment with 1214 µatm pCO_2 in *Acropora nasuta*, while no coral mortality was observed in the other treatments in both coral species. The buoyant weights of 2 coral species increased with incubation time, with net calcification rates ranging from 0.003 to 0.007% d^{-1} (Fig. 4A,B). No tank effects were observed ($F = 0.13$, df = 2, p = 0.88). The net calcification rates of *A. nasuta* (0.006% d^{-1}) were higher than those of *Pocillopora damicornis* (0.004% d^{-1}) in the control group (Fig. 4C,D). The net calcification rates of *A. nasuta* did not change significantly at 700 µatm pCO_2 (only a 3% increase) ($F = 5.69$, df = 2, p = 0.08) but decreased by 18% at 1214 µatm pCO_2 relative to the control (pCO_2 = 389 µatm) during the first 17 d (Fig. 4E). During the entire 94 d experiment, the net calcification rates of *A. nasuta* decreased significantly relative to the control by 29% and 45% under 700 and 1214 µatm pCO_2, respectively ($F = 11.06$, df = 2, p = 0.002) (Fig. 4E). In contrast, the net calcification rates of *P. damicornis* increased by ~60% at both 700 and 1214 µatm pCO_2 over the first 17 d, but over the course of the entire experiment (94 d), the increase was only 20 and 12%, respectively (Fig. 4F).

When the short and mid-term responses were analyzed separately, these 2 coral species also showed different responses to elevated pCO_2. The negative effect of elevated pCO_2 on net calcification rates of *Acropora nasuta* increased from 20% in Days 0 to 17 to 50% during the later stage of the incubation (i.e. Days 17 to 94) ($F = 7.06$, df = 2, p = 0.04) (Fig. 4F). In contrast, elevated pCO_2 greatly increased the net calcification rates of *Pocillopora damicornis* by 60% in Days 0 to 17 of the incubation ($F = 6.86$, df = 2, p = 0.05), but calcification under elevated pCO_2 did not significantly differ from the control during Days 17 to 94 of the incubation ($F = 1.96$, df = 2, p = 0. 45) (Fig. 4F).

Effects of elevated pCO_2 on coral calcification and skeletal stable isotopes ($\delta^{13}C$ and $\delta^{18}O$)

Elevated pCO_2 did not significantly alter the skeletal $\delta^{18}O$ in *Acropora nasuta* ($F = 1.05$, df = 2, p = 0.25), but skeletal $\delta^{18}O$ increased in the pH 7.8 treatment and decreased under pH 7.6 in *Pocillopora damicornis*, suggesting that $\delta^{18}O$-regulating mechanisms are complicated. In contrast, $\delta^{13}C$ decreased from −5‰ in the control to −6.5‰ in the pH 7.6 and 7.8 treatments of *P. damicornis* and decreased from −1‰ in the control to −4‰ in *A. nasuta* (Fig. 5). $\delta^{13}C$ was higher in *P. damicornis* than *A. nasuta* in all the treatments ($F = 8.06$, df = 2, p = 0.02).

Compared to the study by McConnaughey (1989), $\delta^{18}O$ was more deficient in the skeleton of both coral species, while $\delta^{13}C$ was in the range of these historic data (Fig. 5). The $\delta^{13}C$ vs. $\delta^{18}O$ relationship in both *Acropora nasuta* and *Pocillopora damicornis* deviated from that in the non-photosynthetic coral *Tubastrea* sp. (Fig. 5).

DISCUSSION

Acidification effects on coral calcifications

In Sanya Bay, seawater Ω_A was rarely <3.3 (Table 1), and Zhang (2012) also showed that seawater Ω_A in Sanya Bay was >2.5 all the year round. Coral reefs in the modern ocean are believed to be restricted to regions where Ω_A exceeds 3.3 (Kleypas et al. 1999), although cold-water corals can grow in waters with an aragonite saturation close to 1 (Form & Riebesell 2012). The normal Ω_A is predicted to drop down to 2.2 and 1.2 if atmospheric pCO_2 increases to 700 and 1200 µatm respectively in Sanya Bay (Fig. 6). Hence, it is reasonable to expect that elevated atmospheric pCO_2 at the end of this century (>700 µatm) will inhibit coral formation in Sanya Bay as carbonate concentration and Ω_A decrease (Fig. 6). In our study, the 2 coral species exhibited distinctly different responses to elevated pCO_2, even though both were

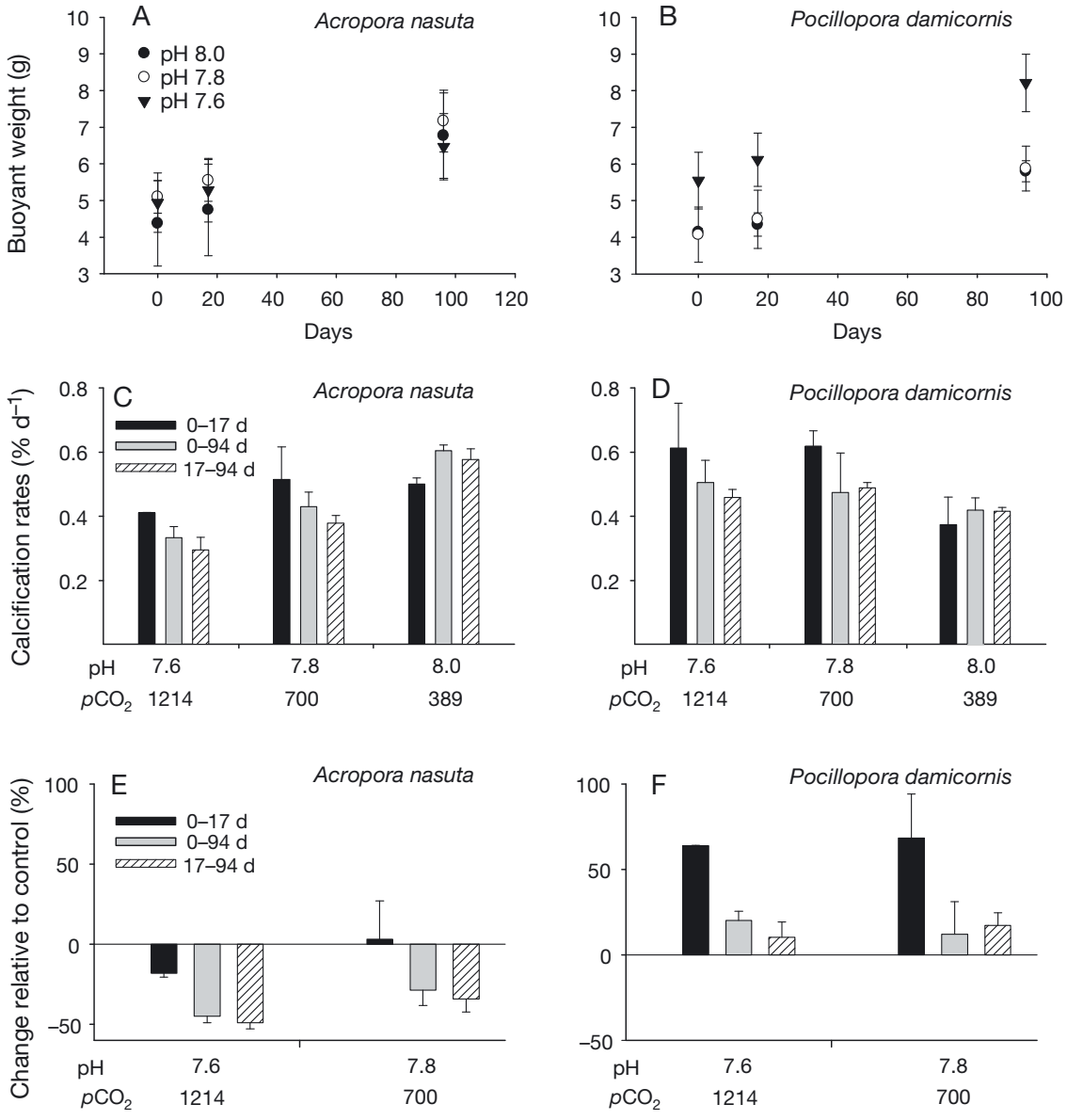

Fig. 4. Coral buoyant weights of 2 coral species: (A) *Acropora nasuta* and (B) *Pocillopora damicornis*; calcification rates of (C) *Acropora nasuta* and (D) *Pocillopora damicornis* in responses to different pH (7.6, 7.8, and 8) when exposed to different pCO_2 levels (389, 700, and 1214 µatm) over Days 0 to 17, 0 to 94, and 17 to 94; percentage change of calcification rates relative to the control in (E) *Acropora nasuta* and (F) *Pocillopora damicornis*. Control is pH 8. Error bars: ± 1 SD

found in the same natural habitats and were cultured under exactly the same conditions.

Acropora nasuta exhibited a decrease in net calcification rate due to elevated pCO_2 during the 94 d incubation (Fig. 4C), which was consistent with findings from previous laboratory and mesocosm experiments showing decreases in calcification with elevated pCO_2 in reef-building corals (Gattuso et al. 1999, Langdon & Atkinson 2005, Marubini et al. 2008). In addition, the negative effects of elevated pCO_2 on net calcification rates were more severe during the later incubation period than the earlier portion (Fig. 4). In contrast, net calcification rates of *Pocillopora damicornis* had a positive response to elevated CO_2 exposure (Fig. 4C). This is at odds with the general consensus that increased pCO_2 reduces calcification in tropical corals (Gattuso et al. 1999, Kleypas et al. 1999). There are fewer studies reporting a positive relationship between pCO_2 and coral calcification, especially in tropical water, although a study on cold-water coral *Lophelia pertusa* in temperate waters showed that elevated pCO_2 insignificantly increased coral calcifi-

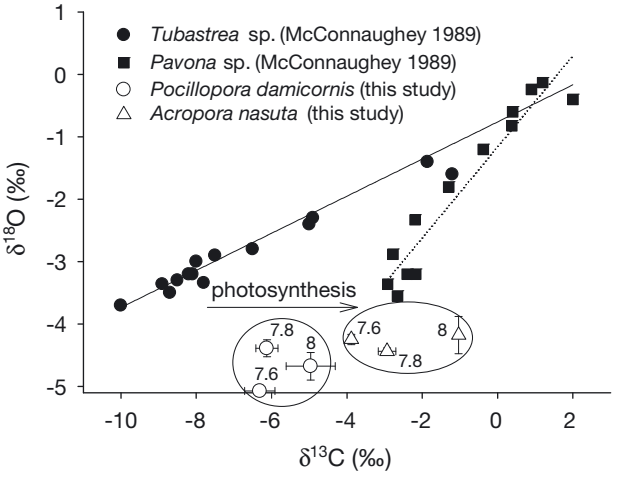

Fig. 5. Skeletal $\delta^{13}C$ versus $\delta^{18}O$ in comparison with the historic data of McConnaughey (1989). The symbols in the circles represent the data corresponding to pH 8, 7.8, and 7.6 treatments in our incubation experiments

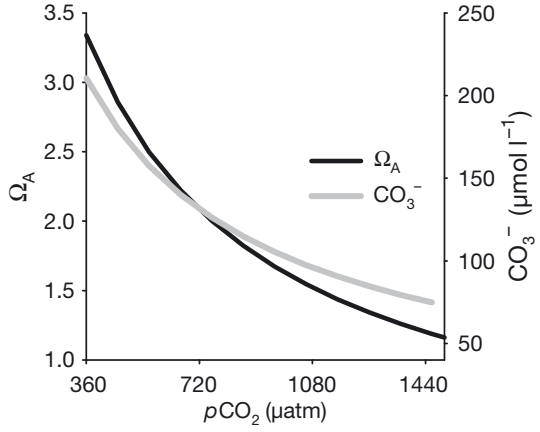

Fig. 6. Modelling data: degree of $CaCO_3$ saturation (Ω_A) and CO_3^{2-} concentrations vary with different seawater pCO_2 levels (360 to 1450 µatm)

cation (Form & Riebesell 2012). Wicks & Roberts (2012) also concluded that the majority of calcification responses to ocean acidification are negative in benthic invertebrates, with the changes in calcification rates ranging from a 99% decline to a 400% increase from a pH drop of 0.3 to 0.5 units. The positive response of *P. damicornis* to elevated pCO_2 was only significant during Days 0 to 17 of the incubation, not during Days 17 to 94 (i.e. relatively long term) (Fig. 4C). This is consistent with the finding that the upregulation of calcification, potentially ameliorating some of the effects of increased acidity, comes at a substantial cost and is therefore unlikely to be sustainable in the long term (Wood et al. 2008). Our results emphasize the need to consider the long-term effects of ocean acidification on organisms with long life-spans, such as corals.

The same coral species, *Pocillopora damicornis*, was also studied in Panamá by Manzello (2010) and appeared to be susceptible to acidification, which is contradictory to our results. However, the results from Panamá were based on historical data collected from *in situ* investigations from 1974 to 2006, which employed different methods than those in our study. Furthermore, the contradictory results may also be due to different coral physiological status and environmental conditions. *P. damicornis* has been found in some coastal waters influenced by riverine inputs with relatively low pH and salinity conditions, such as the coastal waters adjacent to the Pearl River estuary in the northern South China Sea. Notably, no *Acropora nasuta* is present there (H. Huang unpubl. data), although both of the species were present in Sanya Bay. Although pH may be one of the factors influencing coral distribution, it is problematic to conclude that the different distribution of the 2 coral species is directly due to pH variations as there are other regulating factors on corals, such as food supply, temperature, and salinity. Nevertheless, it is possible that the different adaptation of coral species to pH may result in a shift in coral communities in the future, and the different sensitivities to accelerating climate change will be a fundamental determinant of coral reef community structure (Manzello 2010).

Acidification effects on coral photosynthesis

In the present study, coral photosynthesis rate was not directly measured. However, the regression of $\delta^{13}C$ vs. $\delta^{18}O$ has proved to be an effective proxy of the coral photosynthesis. McConnaughey (1989) suggested that photosynthesis could result in higher skeletal $\delta^{13}C$ for a given degree of ^{18}O disequilibrium, and skeletal $\delta^{13}C$ could be increased due to coral photosynthesis. The earlier data from McConnaughey (1989) were included in Fig. 5, showing that the relationship of $\delta^{13}C$ vs. $\delta^{18}O$ in our study was quite different from the relation in non-photosynthetic coral (*Tubastrea* sp.) due to active photosynthesis. In addition, more $\delta^{13}C$ deviation was observed in *Acropora nasuta* than in *Pocillopora damicornis*, suggesting that photosynthesis was higher in *A. nasuta*.

In addition to photosynthesis, acidification may also influence skeletal $\delta^{13}C$, since Fig. 5 showed that $\delta^{13}C$ decreased due to elevated CO_2. A possible explanation for the decrease of $\delta^{13}C$ is the fact that gaseous CO_2 has a smaller fraction of ^{13}C (more negative) than carbonate and bicarbonate in the seawater, and enhanced gaseous CO_2 consequently

resulted in a smaller fraction of ^{13}C entering the coral skeleton. Since skeletal $\delta^{13}C$ would increase due to coral photosynthesis (McConnaughey 1989), the decreases in coral photosynthesis could also be a possible explanation for the lower $\delta^{13}C$ in the pH 7.6 and 7.8 treatments. Unfortunately, we cannot distinguish between the effects of coral photosynthesis and less ^{13}C in gaseous CO_2 in the pH 7.6 and 7.8 treatments.

Model prediction under constant DIC (Scenario 1)

Ries (2011) proposed an H^+-pumping model in which marine calcifiers remove protons (H^+) from their calcifying fluid (internal H^+) and maintain a constant external:internal H^+ ratio between the external seawater and the calcifying fluid under varying atmospheric pCO_2 levels. The coral external:internal H^+ ratio estimated in that study was ~90:1 based on a pH microelectrode measurement (Ries 2011).

This H^+-pumping model was used in our study to show how calcifying fluid Ω_A varies with different levels of pCO_2 when coral external:internal H^+ ratios change (Fig. 7A). This model shows that Ω_A in the calcifying fluid would increase in response to elevated atmospheric pCO_2 when the coral's external:internal H^+ ratio is 100:1, while Ω_A decreases rapidly with elevated pCO_2 when the coral's external:internal H^+ ratio is <2:1 (Fig. 7A). Therefore, increases in calcification at high pCO_2 can occur in this model if the organism exerts strong control over its calcifying fluid pH (e.g. with stronger H^+-pump), as indicated in Scenario 1 (Fig. 7A). However, it seems that an extremely high H^+-pumping efficiency will be required to have a positive response to pH decrease, which comes with a price of energy consumption and is thus less desirable (Ries 2011).

Model prediction under variable DIC (Scenario 2)

The boron isotope studies showed that the calcifying fluid pH of aragonitic corals exhibited a species-dependent range from 8.4 to 8.7 at a typical seawater pH of ~8.1, representing a systematic increase in calcifying fluid pH relative to ambient sea water of ~0.3 to 0.6 units (Anagnostou et al. 2012, McCulloch et al. 2012a). Based on the increases of ~0.3 to 0.6 pH units, the external:internal H^+ ratios are estimated to be ~2:1 to 4:1. However, the studies using microelectrodes and pH-sensitive dyes indicate enhanced calcifying fluid pH by ~0.6 to 1.2 (and possibly up to 2) above seawater during the daytime (Furla et al. 2000,

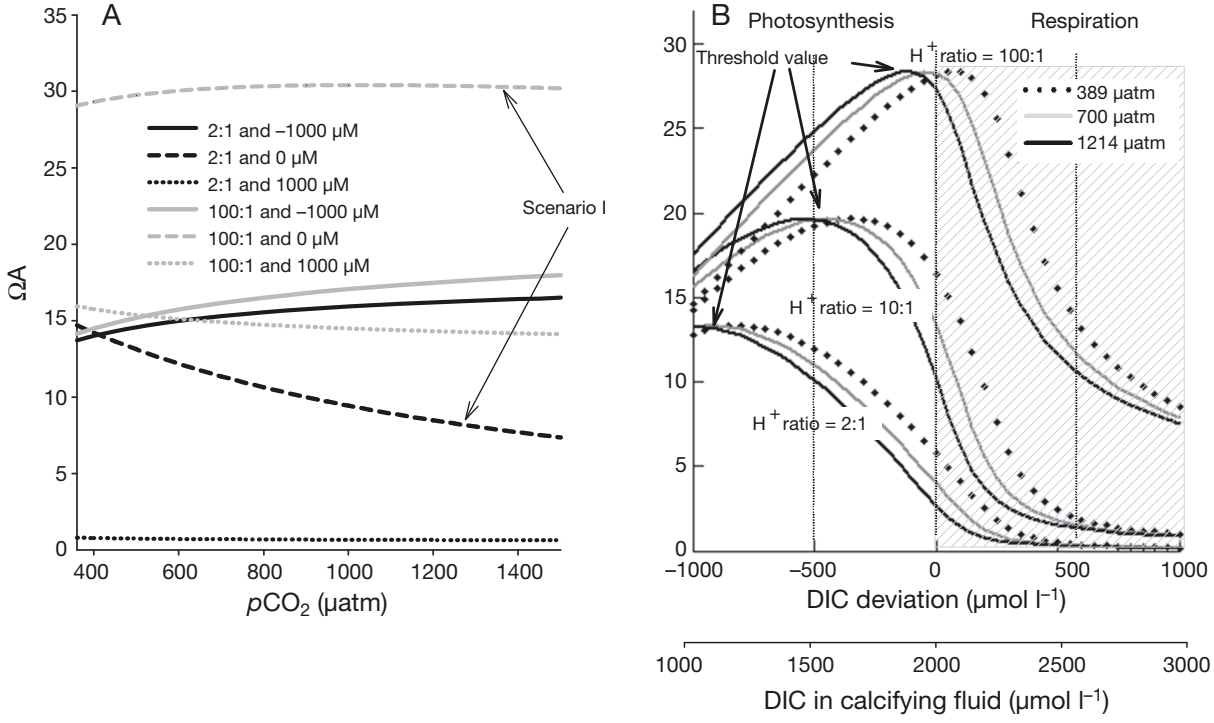

Fig. 7. (A) Aragonite saturation (Ω_A) varies with pCO_2 when external:internal H^+ ratios were 2:1 or 100:1 in the calcifying fluid, coupled with different net dissolved inorganic carbon (DIC) deviations (–1000, 0, and 1000 µmol l^{-1}), respectively. (B) Ω_A varying with different net DIC deviation (ΔDIC) when external:internal H^+ ratios were 2:1, 10:1, or 100:1 under 389, 700, and 1214 µatm, respectively

Al-Horani et al. 2003, Venn et al. 2009, 2011), which represented external:internal H^+ ratios of ~4:1 to 100:1. Hence, the external:internal H^+ ratios are variable due to species and measurement differences.

However, there is still less information about DIC and Ca^{2+} concentrations in calcifying fluid. The modeling data showed that DIC in calcifying fluid varied from 600 to 800 µM (Hohn & Merico 2012), or ~1000 to 2100 µM in the light (Nakamura et al. 2013). In addition, McCulloch et al. (2012a) assumed $DIC_{cf} = 2 \times DIC_{sw}$ and $[Ca^{2+}]_{cf} = [Ca^{2+}]_{sw} + 0.5$ (mmol kg^{-1}) in their model calculations, in which DIC_{cf} and $[Ca^{2+}]_{cf}$ were the DIC and calcium concentrations in calcifying fluid and DIC_{sw} and $[Ca^{2+}]_{sw}$ in seawater, respectively. Therefore, there was still no consensus on DIC concentrations in calcifying fluid, and DIC concentrations in calcifying fluid could be very dynamic due to coral photosynthesis and respiration.

Based on those previously suggested values of DIC (Hohn & Merico 2012, Nakamura et al. 2013), a broad range of DIC concentrations in calcifying fluid was assumed in Scenario 2 with ΔDIC from −1000 to 1000 µmol l^{-1} (Fig. 7). As a direct modification of Scenario 1, Fig. 7 shows that the responses of Ω_A to pCO_2 can sharply differ at different DIC concentrations in calcifying fluid. The relationship between Ω_A and pCO_2 is reversed from positive to negative when ΔDIC varies from −1000 to 1000 µmol l^{-1}. Similarly, when the external:internal H^+ ratio is 2:1, ΔDIC = −1000 µmol l^{-1} due to high photosynthesis also results in a positive relationship between Ω_A and pCO_2, which is reversed when ΔDIC increases to 1000 µmol l^{-1} (Fig. 7). Fig. 7B shows how Ω_A in the calcifying fluid varies with DIC and ΔDIC. When DIC in calcifying fluid reaches a threshold value, Ω_A also reaches a maximum value. Interestingly, when DIC decreases below the threshold value, higher pCO_2 enhances Ω_A in the calcifying fluid, which is favorable to coral calcification (Fig. 7B).

Since measuring net calcification fails to disentangle the relative contributions of gross calcification and dissolution rates on growth (Rodolfo-Metalpa et al. 2011), gross calcification and dissolution should be estimated separately. The empirical exponential rate-dependence law for abiotic carbonate precipitation can be used to calculate net calcification and dissolution with the following equations (McCulloch et al. 2012b):

$$R_{cal} = k_{cal} (\Omega_{Acal} - 1)^n \quad (1)$$

$$k_{cal} = -0.0177T^2 + 1.47T + 14.9 \quad (2)$$

$$n = 0.0628T + 0.0985 \quad (3)$$

$$R_{dis} = k_{dis} (1 - \Omega_{Asw})^n \quad (4)$$

in which R_{cal} and R_{dis} are the gross calcification and dissolution rates of aragonite respectively, k_{cal} and k_{dis} are the rate law constants, Ω_{Acal} and Ω_{Asw} are Ω_A in calcifying fluid and seawater respectively, n is the order of the reaction for aragonite, and T is temperature (Walter & Morse 1985, Burton & Walter 1987). Since Ω_{Asw} was >1 even when pCO_2 is 1400 µatm (Fig. 6), dissolution rates were negligible based on the estimation according to the above equations. With these equations and Ω_A in Fig. 7, net calcification rates could be estimated (Fig. 8). Unfortunately, coral surface areas were not measured in our experiments; hence, the comparison of calcification per surface areas could not be conducted between the experimental and model results. Nevertheless, Fig. 9A indicates that net calcification rates were enhanced by ~20 to 50% due to the increased pCO_2 when DIC was 1000 µM (ΔDIC = −1000 µM) and the external:internal H^+ ratio was 2:1 and 100:1. There would be no coral calcification when the external:internal H^+ ratio was 2:1 and DIC was 3000 µM (ΔDIC = 1000 µM), and hence this data line is not present in Fig. 8A.

Implications for different responses of coral to acidification

Most of the previous studies showed that the responses of coral calcification to acidification are negative (Wicks & Roberts 2012), although the response may change between and within species, and stimulation/inhibition of calcification ranged from +23 to −78% (Erez et al. 2011). The overwhelming number of negative responses reported may imply that DIC in calcifying fluid is often higher than the threshold DIC value or that the pH in calcifying fluid was not high enough due to a weak H^+ pump (Fig. 8B). Meanwhile, positive responses of coral calcification to ocean acidification are possible according to our model of Scenario 2, as the dynamic variation in DIC could cause a different response of coral calcification to elevated CO_2. The dynamic DIC concentrations in coral micro-environment, tissue, and calcifying fluids is caused by active coral photosynthesis (Furla et al. 2000, Al-Horani et al. 2003), which has shown different responses to acidification in different previous studies (Langdon et al. 2003, Schneider & Erez 2006, Marubini et al. 2008, Brading et al. 2011).

Our model provides an explanation for different responses of coral calcification to acidification, but this model did not incorporate the possible relationship between ΔDIC and the H^+ pump. It is possible that coral species with higher photosynthesis rates usually

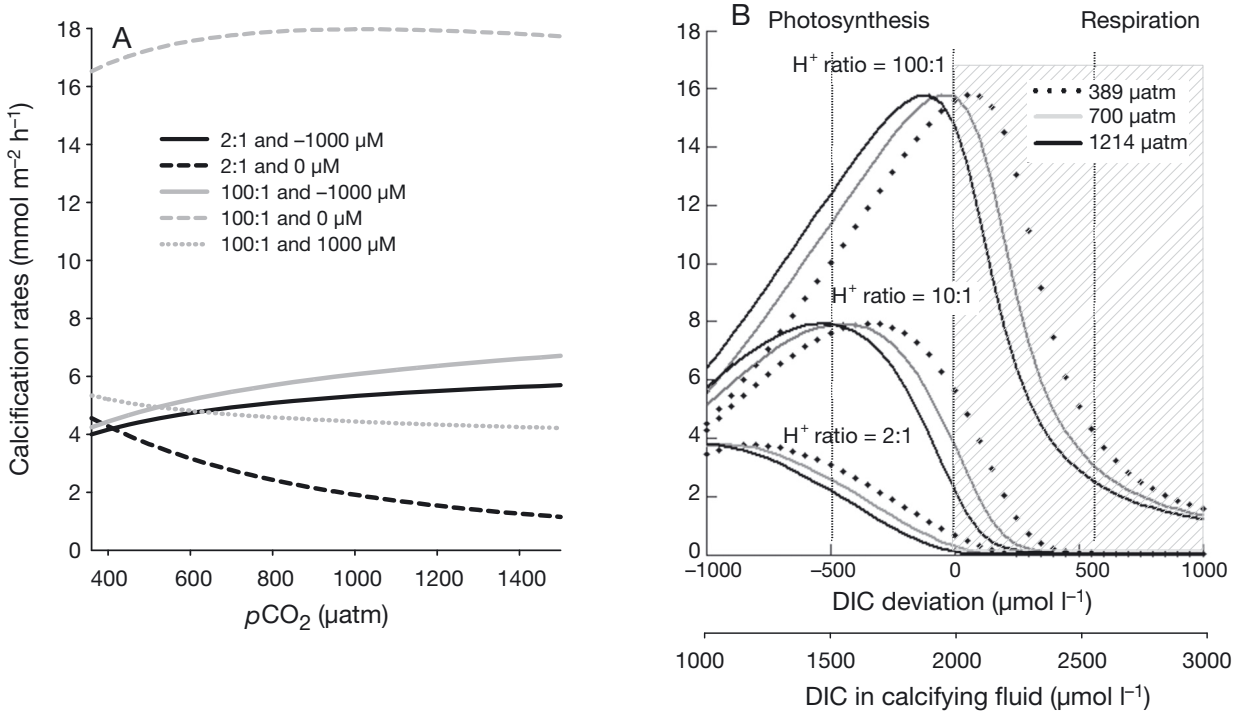

Fig. 8. (A) Calcification rates vary with pCO_2 when external:internal H^+ ratios were 2:1 or 100:1 in the calcifying fluid, coupled with different net dissolved inorganic carbon (DIC) deviations (–1000, 0, and 1000 µmol l^{-1}), respectively. (B) Ω_A varying with different net DIC deviation (ΔDIC) when external:internal H^+ ratios were 2:1, 10:1, or 100:1 under 389, 700, and 1214 µatm, respectively

have stronger H^+ pumps, as photosynthesis provides additional energy for H^+ regulation at the site of calcification. In addition, for marine phytoplankton, photosynthesis increases TA in a ratio of –17:106 to DIC decrease (Cai et al. 2011), but it is not clear whether such ratio is applicable to the internal fluid of a coral. All of these factors need to be further examined by monitoring carbonate parameters in calcifying fluids as well as in the coral microenvironment.

Acknowledgements. We acknowledge the support from the NSFC Project (31370499, 41106107, 31370500, 41076096, 41106141, and 40830850), LMEB201001, CAS program (XDA11020204), and the Ocean Public Welfare Scientific Research Project (201005012-6). The modelling part of this work was partially supported by a NSF grant (EF-1041070) to W.J.C. We thank Dr. B. M. Hopkinson and X.-P. Hu for their helpful comments.

LITERATURE CITED

Al-Horani FA, Al-Moghrabi SM, de Beer D (2003) Microsensor study of photosynthesis and calcification in the scleractinian coral, *Galaxea fascicularis*: active internal carbon cycle. J Exp Mar Biol Ecol 288:1–15

Anagnostou E, Huang KF, You CF, Sikes EL, Sherrell RM (2012) Evaluation of boron isotope ratio as a pH proxy in the deep sea coral *Desmophyllum dianthus*: evidence of physiological pH adjustment. Earth Planet Sci Lett 349–350:251–260

Brading P, Warner ME, Davey P, Smith DJ, Achterberg EP, Suggett DJ (2011) Differential effects of ocean acidification on growth and photosynthesis among phylotypes of *Symbiodinium* (Dinophyceae). Limnol Oceanogr 56: 927–938

Burton EA, Walter LM (1987) Relative precipitation rates of aragonite and Mg calcite from seawater: temperature or carbonate ion control? Geology 15:111–114

Cai W, Hu X, Huang W, Murrell MC and others (2011) Acidification of subsurface coastal waters enhanced by eutrophication. Nat Geosci 4:766–770

Cohen AL, Holcomb M (2009) Why corals care about ocean acidification: uncovering the mechanism. Oceanography (Wash DC) 22:118–127

Crawley A, Kline DI, Dunn S, Anthony K, Dove S (2010) The effect of ocean acidification on symbiont photorespiration and productivity in *Acropora formosa*. Global Change Biol 16:851–863

Dickson AG, Sabine CL, Christian JR (2007) Guide to best practices for ocean CO_2 measurements. PICES Spec Publ 3, Sidney, BC

Erez J, Reynaud S, Silverman J, Schneider K, Allemand D (2011) Coral calcification under ocean acidification and global change. In: Dubinsky Z, Stambler N (eds) Coral reefs: an ecosystem in transition. Springer, New York, NY, p 151–176

Feely RA, Sabine CL, Lee K, Berelson W, Kleypas J, Fabry VJ, Millero FJ (2004) Impact of anthropogenic CO_2 on the $CaCO_3$ system in the oceans. Science 305:362–366

Form AU, Riebesell U (2012) Acclimation to ocean acidification during long-term CO_2 exposure in the cold-water coral *Lophelia pertusa*. Glob Change Biol 18:843–853

Furla P, Galgani I, Durand I, Allemand D (2000) Sources and mechanisms of inorganic carbon transport for coral calcification and photosynthesis. J Exp Biol 203:3445–3457

Gattuso JP, Allemand D, Frankignoulle M (1999) Photosynthesis and calcification at cellular, organismal and community levels in coral reefs: a review on interactions and control by carbonate chemistry. Am Zool 39:160–183

Hoegh-Guldberg O, Mumby PJ, Hooten AJ, Steneck RS and others (2007) Coral reefs under rapid climate change and ocean acidification. Science 318:1737–1742

Hohn S, Merico A (2012) Modelling coral polyp calcification in relation to ocean acidification. Biogeosciences 9: 4441–4454

Hughes TP, Huang H, Young MA (2012) The wicked problem of China's disappearing coral reefs. Conserv Biol 27: 261–269

IPCC (Intergovernmental Panel on Climate Change) (2007) The physical science basis. Contribution of Working Group I to the Fourth Assessment Report of the Intergovernmental Panel on Climate Change. Cambridge University Press, Cambridge

Kleypas JA, Yates KK (2009) Coral reefs and ocean acidification. Oceanography (Wash DC) 22:108–117

Kleypas JA, Buddemeier RW, Archer D, Gattuso JP, Langdon C, Opdyke BN (1999) Geochemical consequences of increased atmospheric carbon dioxide on coral reefs. Science 284:118–120

Kleypas JA, Feely RA, Fabry VJ, Langdon C, Sabine CL, Robbins LL (2006) Impacts of ocean acidification on coral reefs and other marine calcifiers. A guide for future research. Report of a workshop held 18–20 April 2005, St Petersburg, FL sponsored by NSF, NOAA & USGS

Langdon C, Atkinson M (2005) Effect of elevated pCO_2 on photosynthesis and calcification of corals and interactions with seasonal change in temperature/irradiance and nutrient enrichment. J Geophys Res 110:C09S07, doi:10.1029/2004JC002576

Langdon C, Broecker WS, Hammond DE, Glenn E and others (2003) Effects of elevated CO_2 on the community metabolism of an experimental coral reef. Global Biogeochem Cycles 17:1011, doi:10.1029/2002GB001941

Lewis E, Wallace D (1998) CO2SYS. Carbon Dioxide Information Analysis Center, Oak Ridge, TN

Li S, Yu KF, Shi Q, Chen TR, Zhao MX, Zhao JX (2008) Interspecies and spatial diversity in the symbiotic zooxanthellae density in corals from northern South China Sea and its relationship to coral reef bleaching. Chin Sci Bull 53: 295–303

Manzello D (2010) Coral growth with thermal stress and ocean acidification: lessons from the eastern tropical Pacific. Coral Reefs 29:749–758

Marubini F, Ferrier-Pages C, Furla P, Allemand D (2008) Coral calcification responds to seawater acidification: a working hypothesis towards a physiological mechanism. Coral Reefs 27:491–499

McConnaughey T (1989) ^{13}C and ^{18}O isotopic disequilibrium in biological carbonates: I. Patterns. Geochim Cosmochim Acta 53:151–162

McConnaughey T, Whelan J (1997) Calcification generates protons for nutrient and bicarbonate uptake. Earth Sci Rev 42:95–117

McCulloch M, Falter J, Trotter J, Montagna P (2012a) Coral resilience to ocean acidification and global warming through pH up-regulation. Nature Clim Chang 2: 623–627

McCulloch M, Trotter J, Montagna P, Falter J and others (2012b) Resilience of cold-water scleractinian corals to ocean acidification: boron isotopic systematics of pH and saturation state up-regulation. Geochim Cosmochim Acta 87:21–34

Mucci A (1983) The solubility of calcite and aragonite in seawater at various salinities, temperatures, and one atmosphere total pressure. Am J Sci 283:780–799

Nakamura T, Nadaoka K, Watanabe A (2013) A coral polyp model of photosynthesis, respiration and calcification incorporating a transcellular ion transport mechanism. Coral Reefs 32:779–794

Ries JB (2011) A physicochemical framework for interpreting the biological calcification response to CO_2-induced ocean acidification. Geochim Cosmochim Acta 75:4053–4064

Rodolfo-Metalpa R, Houlbrèque F, Tambutté É, Boisson F and others (2011) Coral and mollusc resistance to ocean acidification adversely affected by warming. Nature Clim Chang 1:308–312

Roy RN, Roy LN, Vogel KM, Porter-Moore C and others (1993) The dissociation constants of carbonic acid in seawater at salinities 5 to 45 and temperatures 0 to 45°C. Mar Chem 44:249–267

Schneider K, Erez J (2006) The effect of carbonate chemistry on calcification and photosynthesis in the hermatypic coral *Acropora eurystoma.* Limnol Oceanogr 51:1284–1293

Spencer Davies P (1989) Short-term growth measurements of corals using an accurate buoyant weighing technique. Mar Biol 101:389–395

Venn AA, Tambutté E, Lotto S, Zoccola D, Allemand D, Tambutté S (2009) Imaging intracellular pH in a reef coral and symbiotic anemone. Proc Natl Acad Sci USA 106:16574–16579

Venn A, Tambutté E, Holcomb M, Allemand D, Tambutté S (2011) Live tissue imaging shows reef corals elevate pH under their calcifying tissue relative to seawater. PLoS ONE 6:e20013

Wallace CC (1999) Staghorn corals of the world: a revision of the coral genus *Acropora* (*Scleractinia*; *Astrocoeniina*; *Acroporidae*) worldwide, with emphasis on morphology, phylogeny and biogeography. CSIRO Publishing, Collingwood

Walter LM, Morse JW (1985) The dissolution kinetics of shallow marine carbonates in seawater: a laboratory study. Geochim Cosmochim Acta 49:1503–1513

Wicks L, Roberts M (2012) Benthic invertebrates in a high-CO_2 world. Oceanogr Mar Biol Annu Rev 50:127–188

Wood HL, Spicer JI, Widdicombe S (2008) Ocean acidification may increase calcification rates, but at a cost. Proc R Soc Lond B Biol Sci 275:1767–1773

Zhang C, Huang H, Ye C, Huang L, Li X, Lian J, Liu S (2013) Diurnal and seasonal variations of carbonate system parameters on Luhuitou fringing reef, Sanya Bay, Hainan Island, South China Sea. Deep-Sea Res II 96:65–74

Zhang J (2012) Impacts of climate change (including sea level rise, warming and ocean acidification) on the marine environment. In: Zhang J, Huang H (eds) Ecosystem issues and policy options addressing the sustainable development of China's ocean and coast. China Environmental Science Press, Beijing, p 440–459

Zhang Q (2007) Responses of tropical biological coasts to global change. Quat Sci Rev 27:834–844 (in Chinese)

Zhang Y, Chen L (2006) Response of coral reef in Nansha waters to increasing atmospheric CO_2. J Oceanogr Taiwan 25:68–76

Editorial responsibility: Karen Miller, Hobart, Tasmania, Australia

Submitted: May 7, 2013; Accepted: January 7, 2014
Proofs received from author(s): March 20, 2014